

An engineering model for prediction of waste incineration in a dump combustor

S. Arunajatesan

Georgia Inst. of Technology, Atlanta

S. Menon

Georgia Inst. of Technology, Atlanta

AIAA, Aerospace Sciences Meeting & Exhibit, 35th, Reno, NV, Jan. 6-9, 1997

An engineering model that can be used to obtain predictions of axial distributions of temperature and species concentrations in complex flows has been formulated and applied to waste incineration in a dump combustor. The model incorporates mean convection and molecular diffusion in a quasi-1D sense and uses a stochastic model to approximate the effects of turbulent convection. The inputs to the model are extracted from experimental data and results of large eddy simulations. Comparisons of waste consumption rates and pollutant formation in the dump combustor with experimental data show that the model can capture the correct trends and achieve fairly good quantitative agreement. Further, the model does not use any ad-hoc constants that need to be calibrated or tuned. (Author)

An Engineering Model for Prediction of Waste Incineration in a Dump Combustor*

S. Arunajatesan[†] and S. Menon[‡]
School of Aerospace Engineering
Georgia Institute of Technology
Atlanta, GA 30332-0150

Abstract

An engineering model that can be used to obtain predictions of axial distributions of temperature and species concentrations in complex flows has been formulated and applied to waste incineration in a dump combustor. The model incorporates mean convection and molecular diffusion in a quasi-one dimensional sense and uses a stochastic model to approximate the effects of turbulent convection. The inputs to the model are extracted from experimental data and results of Large Eddy Simulations (LES). Comparisons of waste consumption rates and pollutant formation in the dump combustor with experimental data show that the model can capture the correct trends and achieve fairly good quantitative agreement. Further, the model does not use any ad-hoc constants that need to be calibrated or tuned.

1 Introduction

There is a strong need in the industry for methods that accurately analyze combustor flows in order to obtain quick solutions to design problems. Simple models or methods capable of predicting mean values without undue computational expense are needed. An additional feature desired of these models is that they should be capable of handling varied flow conditions without requiring recalibration. These models, when developed, can then be used to parameterize the flow in complex geometries with respect to any of the variables of the problem. In this paper, we address this need by developing a simple model to predict complex combustor flows.

Many of the earlier attempts to model com-

plex geometry combustor flows using simplified models have been largely directed towards the control of instabilities that develop in these combustors [1, 2, 3]. Most of these methods use some procedure that simplify the equations (typically, linearization) to obtain equations for the perturbations in the flows. More often than not, this assumes knowledge of the mean flow field information to solve the perturbation equations. Yang and Culick [4] used an integral technique to solve for the mean flow variables and then used this information to solve the linearized perturbation equations. However, this analysis was used to mainly study the modes of acoustics and instabilities in a liquid fueled ramjet. In another work, Logan et al. [5] analyzed the acoustic modes of a low speed dump combustor. Again, the mean flow field information was assumed known rather than calculated. In an earlier work, Jou and Menon [2] used the information obtained from numerical simulations to construct a model for the pressure oscillations in a ramjet. , Sterling et al. [6] studied the longitudinal mode instabilities in a dump combustor using experimental measurements. Thus, although significant amount of work has been directed towards the phenomena of instabilities and pressure oscillations in combustor flows, relatively little effort has gone into developing simple models to predict the mean reacting flow fields in these combustors.

In this paper, results from an ongoing research initiative to develop an engineering model to study complex combustor flows are presented. The model is being developed to study the controlled incineration of toxic wastes in a dump combustor. This approach parallels an ongoing experimental study of an identical dump combustor [19]. The basic model formulation and details are presented in the next section. The model uses the concept of stochastic stirring events to model the effects of turbulent stirring, first postulated by Kerstein [12], in conjunction with a quasi-one dimensional solver.

*Copyright ©1997 by S. Arunajatesan and S. Menon. Published by the American Institute of Aeronautics and Astronautics, Inc., with permission.

[†]Graduate Research Assistant, Student Member, AIAA

[‡]Associate Professor, Senior Member, AIAA

The model uses as input, parameters that describe the turbulence in the flow field such as, the integral length scale variation and the rms of the velocity fluctuations. These parameters are obtained from experimental measurements of the turbulent flow field. The parameters governing the stirring events are derived based on three dimensional scaling laws for homogeneous turbulence.

2 Model Formulation

In the approach adopted here, the turbulent flow field in a dump combustor is conceptually broken down into the various physical processes occurring in the combustor shear layer. The processes considered are the following : 1) Mean convection at the convection velocity of the structures in the shear layer, 2) The turbulent convection/stirring due to the presence of vortices in the shear layer, 3) Molecular diffusion due to the presence of scalar gradients, and 4) chemical reaction and the accompanying heat release. Each one of these physical processes is handled distinctly and these various models and their relevant parameters are discussed below.

The mean convection of the scalars in the shear layer is handled using the quasi-one dimensional equations. The reduced convection velocities in the shear layer are modeled as the effects of area changes. It should be noted here that we are interested only in modeling the turbulent mean flow and not the unsteady flow variations. Thus, by using either full numerical simulation or experimental measurements (as is done here) the target velocity profiles are known apriori. The area distribution is adjusted until the mean flow velocity profile is obtained. Large variations are not expected in the mean velocity profiles for small changes in the operating parameters of the system. Hence, this calibration is expected to be required only once for a given geometry.

The second aspect concerns modeling of fuel-air mixing. Fuel injection is modeled as simple mass addition into the variable area flow. This gives rise to source terms in the governing equations for mass, momentum, energy, and mass fractions of the species. Mixing is modeled in two parts. Molecular mixing is accounted for by directly including the diffusive terms in the governing equations for the quasi-one dimensional flow. Fickian diffusion is assumed for the species and, in this work, all the species are assumed to have equal diffusivities and unity Lewis number although the formulation is generic .

Turbulent stirring is accounted for by the

stochastic stirring events that mimic the action of an eddy on a scalar field. This is done by random rearrangement events of the scalar field along the domain. The laws governing these rearrangements are derived such that the apparent diffusion induced by these processes mimic that experienced by a particle in a real turbulent flow. In order to do this, the high Reynolds number scalings based on the Kolmogorov cascade are used. The stirring events can then be described in terms of two parameters. The first one is a stirring frequency parameter (λ) which determines the rate at which these stirring events occur. The second parameter is a pdf describing the size distribution of the rearrangement events. The actual expressions for these parameters depend on the kind of mapping event chosen. In this study the block inversion mapping is chosen. Mathematically, the block inversion mapping of an arbitrary scalar field $\theta(x, t)$ can be expressed as follows,

$$\theta(x, t) = \begin{cases} \theta(2l_0 - x, t) & \text{if } l_0 - l < x < l_0 + l \\ \theta(x, t) & \text{otherwise} \end{cases} \quad (1)$$

Detailed description of the mapping and its diffusive and dispersive properties are discussed by Kerstein [12] and are omitted here for brevity. Using the derivations given there, the following expressions are derived,

$$\lambda = \frac{24 \nu R_{e,L}}{5 \eta^3} \frac{1 - (L/\eta)^{-5/3}}{(L/\eta)^{4/3} - 1} \quad (2)$$

$$f(l) = \frac{5}{3} \frac{L^{-8/3}}{\eta^{-5/3} - L^{-5/3}} \quad (3)$$

where, ν is the kinematic viscosity, L is the integral length scale, $R_{e,l}$ is the Reynolds number based on the rms velocity fluctuations and the integral length scale, and η is the kolmogorov length scale. Note that, in general, since L and u_{rms} are also a functions of space, both λ and $f(l)$ are in general functions of space.

The quasi-one dimensional equations are marched in time. When the epoch for a stirring event occurs, the location of the event is chosen. In order to do this we define the global event rate $E(t)$ at time t as

$$E(t) = \int \lambda(x, t) dx \quad (4)$$

Now, the event location is selected randomly with probability $\lambda(x, t) dx / E(t)$ that its center falls in the interval $(x, x + dx)$. Once the location is selected, the event size is chosen by randomly sampling

the pdf $f(l)$. Then, the scalar field is subjected to the mapping given in 1. This is done in such a way that equal masses are interchanged between cells undergoing the inversion process. After the inversion at the current time has been completed, the time interval to the next event is determined by sampling an exponential distribution with mean $1/E(t)$. The solver then goes back to the quasi-one dimensional system until that time for the next inversion is reached at which point the above process is again repeated. The aspects of this implementation specific to its application to the shear layer in a dump combustor are discussed later.

The final aspect is the modeling of the chemistry in the combustor. In the cases considered here, a mixture of ethylene and benzene is used as fuel and waste. Ethylene is the actual fuel, while the benzene is used as a waste surrogate. This study is a part of a larger effort to evaluate the use of a dump combustor type geometry for the purpose of waste incineration. In order to evaluate fuel and waste consumption rates in the combustor, a realistic reaction mechanism has to be used. The complete mechanism for the combustion of ethylene consists of 277 reactions involving 48 species[7]. It is computationally forbidding to use this full mechanism. Hence, a methodology suggested by Singh and Jachimowski[8] is used. This reduces the mechanism to a more manageable 11 reactions among 10 species. Pollutant formation in combustors of the type considered here is a major problem that needs to be addressed. Therefore an additional reaction based on the suggestion by Chen and Kollmann[9] for the formation of NOx is used for this purpose. The final reaction system contains 12 species and 12 reactions and is given in Table 1. The coefficients from CHEMKIN [11] chemical kinetics package is used to calculate the free energies for the computation of the reaction rate data.

In the following section, the equations used in the model are presented. The various sub-models described above are discussed in greater detail and methods of their calibration are discussed.

3 Governing Equations

The governing equations are the basic conservation laws for mass, momentum, energy and species mass fractions for a quasi-one dimensional flow with area variation. These equations for a multi-component system are written as follows:

$$\frac{\partial QA}{\partial t} + \frac{\partial FA}{\partial x} = G_A + G_m \quad (5)$$

Reaction	A	n	E_a
$C_2H_4 + 3O_2 \rightleftharpoons 2CO + 2H_2$	2.2e11	0.0	1.5558e8
$C_6H_6 + 3O_2 \rightleftharpoons 6CO + 3H_2$	1.8e8	0.0	1.4859e8
$CO + O \rightleftharpoons CO_2 + M$	5.3e1	0.0	-1.9004e7
$CO + OH \rightleftharpoons CO_2 + H$	4.4	1.5	-3.0975e6
$H_2 + O_2 \rightleftharpoons OH + OH$	1.7e7	0.0	2.0092e8
$H + O_2 \rightleftharpoons OH + O$	2.6e8	0.0	7.0322e7
$OH + H_2 \rightleftharpoons H_2O + H$	2.2e7	0.0	2.1557e7
$O + H_2 \rightleftharpoons OH + H$	1.8e4	0.0	3.7254e7
$OH + OH \rightleftharpoons H_2O + O$	6.3e7	0.0	4.5626e6
$H + H \rightleftharpoons H_2 + M$	6.4e5	-1.0	0.0
$H + OH \rightleftharpoons H_2O + M$	2.2e10	-2.0	0.0
$N_2 + O_2 \rightleftharpoons 2NO$	1.82e8	0.0	1.6061e8

Table 1: Chemical reaction mechanism used in the present work and in the LES simulations

$$Q = \begin{bmatrix} \rho \\ \rho u \\ \rho E \\ \rho Y_k \end{bmatrix} \quad (6)$$

$$F = \begin{bmatrix} \rho u \\ \rho u^2 + p \\ \rho u H \\ \rho Y_k u \end{bmatrix} \quad (7)$$

$$G_A = \begin{bmatrix} 0 \\ p \frac{dA}{dx} \\ 0 \\ \dot{\omega}_k \end{bmatrix} \quad (8)$$

$$G_m = \begin{bmatrix} \frac{dm_e}{dx} \\ u_e \frac{dm_e}{dx} \\ H_e \frac{dm_e}{dx} \\ Y_{k,e} \frac{dm_e}{dx} \end{bmatrix} \quad (9)$$

In the above, ρ is the density, u is the velocity, E is the total energy per unit mass given by,

$$E = e + \frac{u^2}{2} \quad (10)$$

where e is the internal energy per unit mass given by,

$$e = h - \frac{p}{\rho} \quad (11)$$

and

$$h = \sum_{k=1}^{N_s} Y_k h_k \quad (12)$$

$$h_k = \Delta h_{f,k}^\circ + C_{p,k}(T - T_o) \quad (13)$$

Here, A is the area, p is the pressure, H is the total enthalpy per unit mass, Y_k is the mass fraction of the k^{th} species and $\dot{\omega}_k$ is the production

rate of the k^{th} species. The right hand side terms in equation 5 represent the source terms due to area variation, G_A , and mass addition G_m . m_e is the mass flow rate of the injected mass, u_e is the velocity of the injected mass, H_e is the total enthalpy per unit mass of the injected mass and $Y_{k,e}$ is the mass fractions of the k^{th} species.

The governing equations described here are solved by a simple finite difference technique using the explicit second order MacCormack Scheme. The solution is marched time accurately to steady state.

In deriving the equations 2 and 3, it is assumed that all the scales of motion ranging from the smallest Kolmogorov scales to the largest integral length scales occur in the flow[12]-[18]. This implies that in a numerical simulation, the entire range of scales should be completely resolved. However, it has been found that this is not always necessary. Resolving scales larger than approximately 10η has been found to yield sufficiently accurate results[12], [15]. Hence, in the present work also only scales larger than 10η are resolved.

4 Results

A schematic of the dump combustor along with the close up of the injection region is shown in figure 1. Figure 2 shows the schematic of the model that represents the dump. Only the region downstream of the dump plane is modeled. The sudden expansion is modeled as a section with a large increase in area. The dump area then changes again, the diameter dropping to a smaller pipe. This causes the formation of a large recirculation area behind the dump plane. This reduction in area to a smaller pipe is modeled as a straightening of the one dimensional channel with a corresponding decrease in cross sectional area. This kind of modeling of the flow is appropriate because we are only trying to approximate the mean flow field. The actual dump combustor flow field contains an unsteady shear layer which is not of interest here.

In order to determine a starting point for the simulations, the data from an LES of the combustor flow field and the corresponding experimental investigation were used. Figures 3 and 4 show the experimentally measured mean velocity and rms velocity fluctuation profiles in the near field of the dump. The center line of the shear layer is identified as the line of maximum rms velocity. A plot of the mean velocity along this center line is shown in figure 5. Also shown in this figure is the velocity profile obtained by varying the area function in the

model. This mean axial velocity profile is used in all the simulations.

Next, the inputs needed for the stirring model need to be determined. From equations 2 and 3, it is clear that the integral length scale(L) variation needs to be known a priori. In order to calculate this we need to adopt a visualisation of the shear layer behind the dump. The picture of the shear layer adopted in this work is shown in figure 6. In the near field of the dump, the shear layer is assumed to grow linearly, similar to a mixing layer behind a splitter plate. The initial layer thickness and the linear growth rate of the shear layer are extracted from the LES calculations. The LES calculations show that in the near field, the shear layer grows with a slope of about 0.2. This is also confirmed by the experimental velocity profiles 3,4. This thickness and growth rate is based on the vorticity thickness. Since the stirring events represent the action of eddies of different sizes, and, the vorticity thickness represents the maximum size of the vortices found in the shear layer, this value is used for the integral length scale L .

Further downstream in a dump combustor, the shear layer curves towards the wall and reattaches after a certain length. In this region the linear growth rate hypothesis is no longer accurate. However, our experience with this geometry and the experimental results have shown that the primary *action zone* is in the near field of the dump plane and, hence, it is expected that this approximation will not significantly alter the results. Reasonably good agreement with experimental measurements seem to show that this is the case.

Another parameter that needs to be specified is the turbulent Reynolds number. This can be done by specifying the turbulent velocity scale variation in the shear layer. Since the shear layer center line has been assumed to lie along the line of maximum U_{rms} , it would be appropriate to specify the U_{rms} as the turbulent velocity scale in the shear layer. From figure 4, we see that this maximum value is nearly a constant along the length of the shear layer and is around 20% of the mean velocity. Hence, in the present work, the turbulent velocity is specified as a constant 20% of the reference velocity.

The above model formulation was applied to the case of combustion of waste surrogate (Benzene) in a dump combustor. One of the primary quantities of interest in this case is the consumption efficiency, also known as the Destruction and Removal Efficiency (DRE). This is a measure of how quickly the injected waste surrogate is consumed in

the dump. A quantitative measure of this is given by calculating number of nines as follows,

$$\#of9's = -\log_{10}\left(1.0 - \frac{\%consumption}{100}\right) \quad (14)$$

Hence, a consumption of 99.99% yields a DRE of 4.

A plot of the DRE as a function of the non-dimensional axial distance is shown in figure 7. It is seen that the predicted DREs are in reasonable agreement with the experimental data in the near field. Further downstream the DRE's are overpredicted by the model. This is possibly due to various reasons. The chemical mechanism was reduced from a larger, more detailed mechanism and allows for only the breakdown of the benzene molecules. There is now evidence to suggest that benzene may be formed as an intermediary in the combustion of some hydrocarbons. This feature is not included here.

Another reason for this overprediction is the assumption of calorically perfect gas (used here only as an approximation, but can easily be relaxed) used in the caloric equation of state, i.e., the specific heats of the gases are assumed to be constant. These values are assumed to remain constant at their values for a real gas at 300K. However, it is known that the specific heats can change by a factor of almost 3–3.5 in the temperature ranges witnessed in the present case 8. This results in an overprediction of the temperature distribution and hence, results in increased reaction rates and higher consumption rates.

Another reason for this increased reaction rates downstream may be due to the manner in which the rearrangement events that mimic turbulent stirring are implemented. When a certain location is chosen for the stirring event and the size of the stirring event is determined, it is assumed that equal masses are stirred and that these masses carry their temperatures with them. This is done to mimic the increased thermal diffusivity in turbulent flows. However, in the one-dimensional simulations, since there is no *transverse* thermal diffusion this might result in a slight overprediction of the thermal diffusion in the axial direction. This results in higher temperatures in the downstream regions and, hence, higher DRE's.

A very important aspect of hydrocarbon combustion is the emission of pollutants. Efforts are underway to reduce pollution by the emission of dangerous combustion by-products like carbonmonoxide(CO) and oxides of nitrogen(NO_x). In our study, one of the major criteria used to validate the model has been the prediction of pollutant emission. A plot of the carbonmonoxide mass fraction

(in ppm) is shown in figure 9. It is seen that for an equivalence ratio of 0.54 (for which experimental data was available), the model predictions compare very well with the experimental data. Also, not much variation is seen in the near field with change in the equivalence ratio. However, further downstream, significant variation is seen.

A plot of the variation of the CO emission with change in the equivalence ratios is shown in figure 10. Values plotted are the CO mass fraction (again in ppm) at $X/D = 3.0$. The model predictions are in excellent agreement with the experimental results. The CO emission is seen to be minimal around equivalence ratios around 0.85. At lower and higher ratios, the emission is seen to rise significantly. This has experimentally been observed to be caused by a marked decrease in flame stability and increase in its *sootiness* [19]

Figure 11 shows the variation of NO along the non-dimensionalised axial coordinate. The NO production mechanism used in these studies is the reduced Zeldovich mechanism given by Chen and Kollmann[9]. It is seen that the agreement between the model predictions and the experimental data is reasonably good. However, the model slightly overpredicts the NO emission. This is due to the fact that the temperatures are slightly over-predicted as discussed above. This further indicates that the thermally perfect gas model for the caloric equation of state needs to be used. The CO and NO emission are seen to follow very different trends. While CO decreases with downstream distance, NO is seen to increase with X/D . Figure 12 shows the variation in NO emission with equivalence ratio. Again, in contrast to the CO variation discussed earlier, NO emission is seen to increase with increase in ϕ . These trends are captured very accurately by the model.

These results presented here show that the baseline model, as presented here, is capable of capturing the major DRE and emission trends observed in the experimental investigation. However, the global research effort is directed towards the development of an efficient combustor. Results from experiments and LES investigations show that acoustic and mechanical forcing of the combustor flow can significantly increase the combustion efficiency in the combustor[10],[19]. This forcing has also been observed to reduce the CO and NO emission significantly. Our future work will be directed towards incorporating a mechanism to capture these effects into the model presented here.

5 Conclusion

The engineering model developed is seen to be capable of capturing all the correct trends with respect to waste consumption and pollutant formations. In most cases, not only are the qualitative agreements good, but the results compare quantitatively well with experimental data. The model is fairly simple to apply to almost any kind of combustor geometry and has not required any significant calibration or tuning. The inputs to the model are logically extracted from simple experimental and LES results.

References

- [1] Smith, D.A., Zukoski, E.E., Combustion Instability Sustained by Unsteady Vortex Combustion, Twenty first Joint Propulsion Conference, Monterey, CA, Paper 1248, 1985.
- [2] Jou, W.-H., Menon, S., Modes of Oscillation in a Nonreacting Ramjet Combustor Flow, *Journal of Propulsion and Power*, Vol. 6 No. 5, pp 535-543, 1990.
- [3] Wake, B.E., Choi, D., Hendricks, G.J., Numerical Investigation of Pre-Mixed Step Combustor Instabilities, AIAA-96-0816, 1996.
- [4] Yang, V., Culick, F.E.C., Linear Theory of Pressure Oscillations in Liquid-Fueled Ramjet Engines, AIAA-83-0574, 1983.
- [5] Logan, P., Lee, J.W., Lee, L.M., Karagozian, A.R., Acoustics of a Low-Speed Combustor, *Combustion and Flame* Vol. 84, pp 93-109, 1991.
- [6] Sterling, J.D., and Zukoski, E.E. Longitudinal Mode Combustion Instabilities in a Dump Combustor, AIAA-87-0220, 1987.
- [7] Dagaut, P., Cathonnet, M., Boettner, J.C., Gaillard, F., Kinetic Modeling of Ethylene Oxidation, *Combustion and Flame*, Vol. 71, pp 295-312, 1988.
- [8] Singh, D.J., and Jachimowski, C.J., Quasiglobal Reaction Model for Ethylene Combustion, *AIAA Journal* Vol. 32 No.1, pp 213-216, 1994.
- [9] Chen, J.-Y., Kollmann, W., PDF Modeling and Analysis of Thermal NO Formation in Turbulent Nonpremixed Hydrogen-Air Jet Flames, *Combustion and Flame*, Vol. 88, pp 397-412, 1992.
- [10] Arunajatesan, S., Menon, S., Simulation of Controlled Injection of Toxic Waste for Enhanced Destruction in a Compact Incinerator, AIAA-96-3077, 1996.
- [11] Kee, R.J., Rupley, F.M., Miller, J.A., CHEMKIN-II: A Fortran Chemical Kinetics Package for the analysis of Gas Phase Chemical Kinetics, SAND89-8009B, 1993.
- [12] Kerstein, A.R., A Linear-Eddy Model of Turbulent Scalar Transport and Mixing, *Combustion Science and Technology*, Vol. 60, pages 391-421, 1988.
- [13] Kerstein, A.R., Linear-Eddy modeling of Turbulent Transport. II : Application to Shear Layer Mixing, *Combustion and Flame* 75:397-413 (1989)
- [14] Kerstein, A.R., Linear-Eddy modeling of Turbulent Transport. Part 3. Mixing and Differential Molecular Diffusion in round jets, *Journal of Fluid Mechanics*, Vol. 216, pages 411-435 (1990)
- [15] Kerstein, A.R., Linear-Eddy modeling of Turbulent Transport. Part 4. Structure of Diffusion Flames, *Combustion Science and Technology*, Vol. 81, pages 75-96, 1992.
- [16] Kerstein, A.R., Linear-Eddy modeling of Turbulent Transport. Part V: Geometry of Scalar Interfaces, *Physics of Fluids A*, Vol. 3 (5), pages 1110-1114, 1991.
- [17] Kerstein, A.R., Linear-Eddy modeling of Turbulent Transport. Part 6. Microstructure of diffusive scalar mixing fields, *Journal of Fluid Mechanics*, Vol. 231, pages 361-394 (1991)
- [18] Kerstein, A.R., Linear-Eddy modeling of Turbulent Transport. Finite-rate chemistry and multi-stream mixing, *Journal of Fluid Mechanics*, Vol. 240, pages 289-313 (1992)
- [19] Parr, T.P., et.al., Compact Incinerator Afterburner Concept based on Vortex Combustion, *Twenty-Sixth International Symposium on Combustion*, Naples, Italy, 1996.

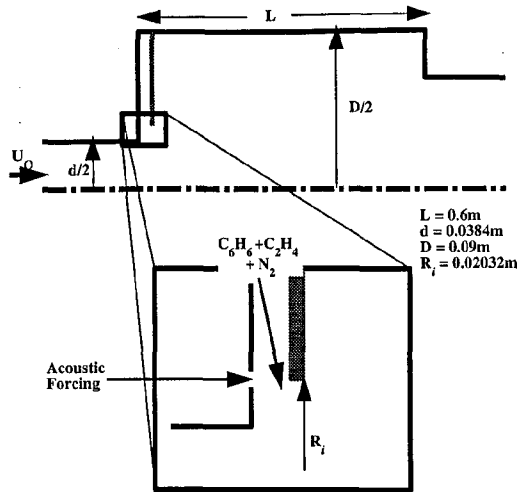


Fig. 1. Schematic of the dump combustor used in the experiments [19] and LES.

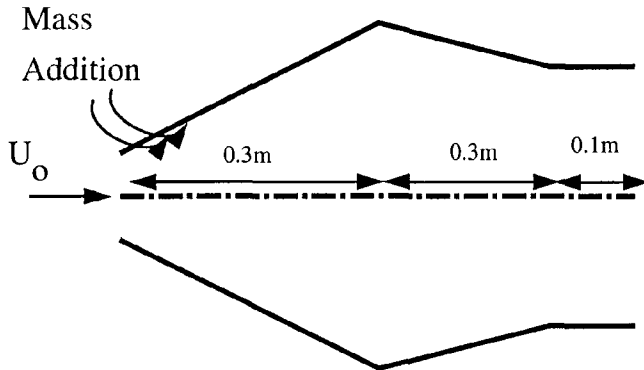


Fig. 2. Schematic of the model geometry used in the present work.

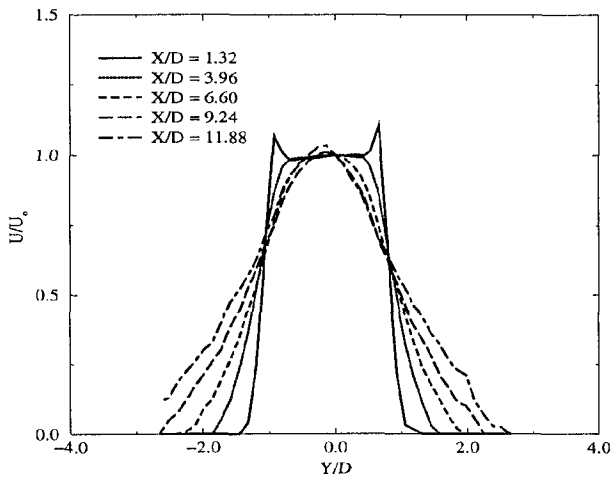


Fig. 3. Mean axial velocity profiles measured experimentally in the dump combustor [19].

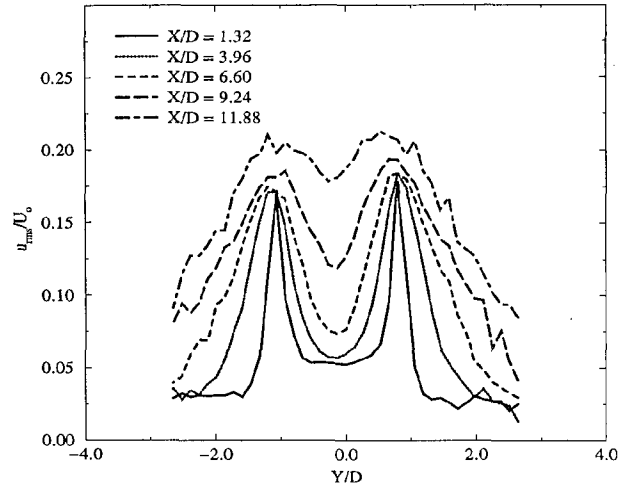


Fig. 4. Axial rms velocity profiles measured experimentally in the dump combustor [19]

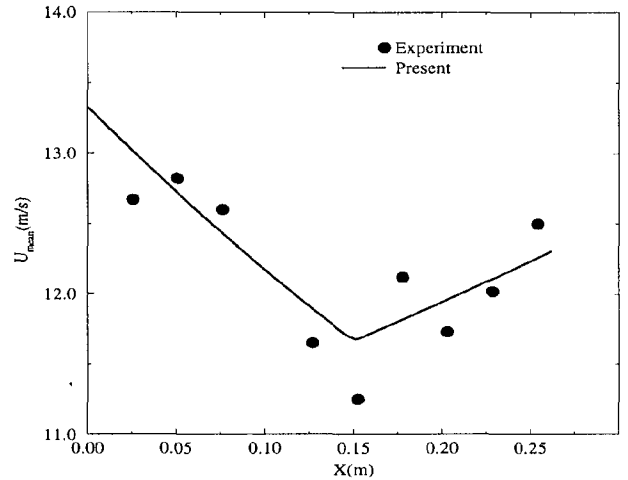


Fig. 5. Mean axial velocity along the shear layer centerline

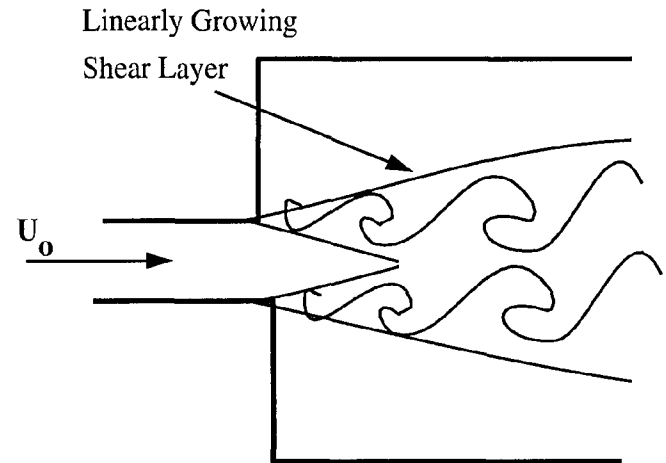


Fig. 6. Topology of the shear layer used in the present work.

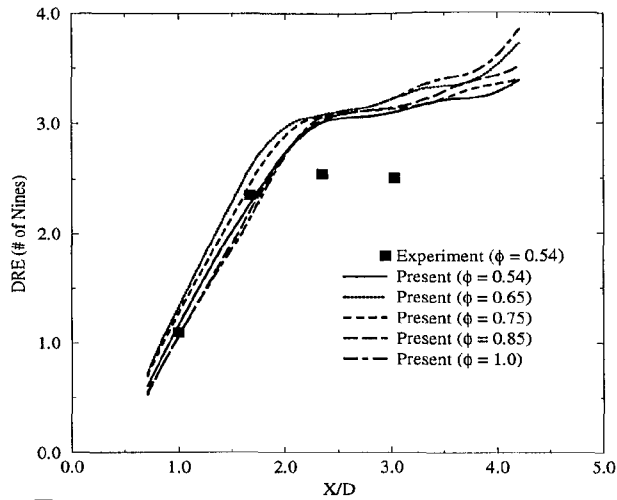


Fig. 7. Comparison of the Benzene DRE variation along the axial co-ordinate with the experimental data.

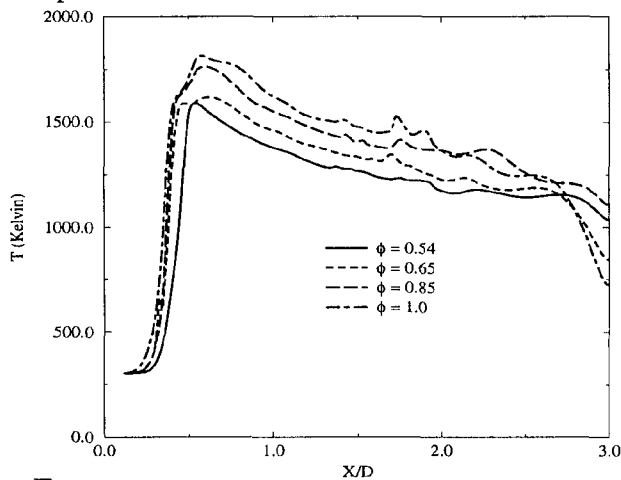


Fig. 8. Temperature profiles predicted by the model using the calorically perfect gas model.

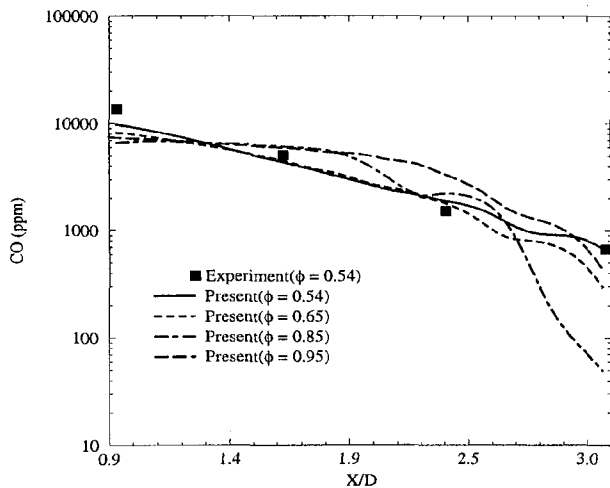


Fig. 9. CO variation along the axial coordinate

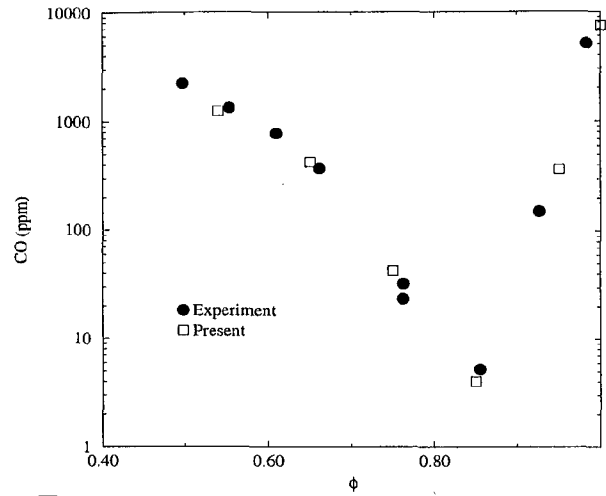


Fig. 10. CO mass fraction variation with ϕ . Measurements at X/D = 3.0 are shown

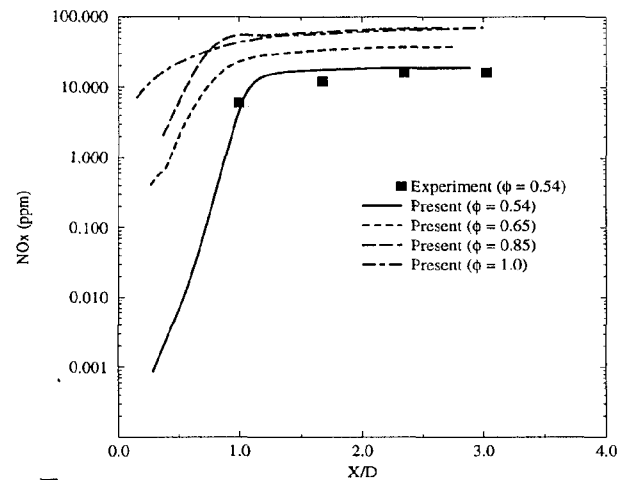


Fig. 11. NO variation along the axial coordinate.

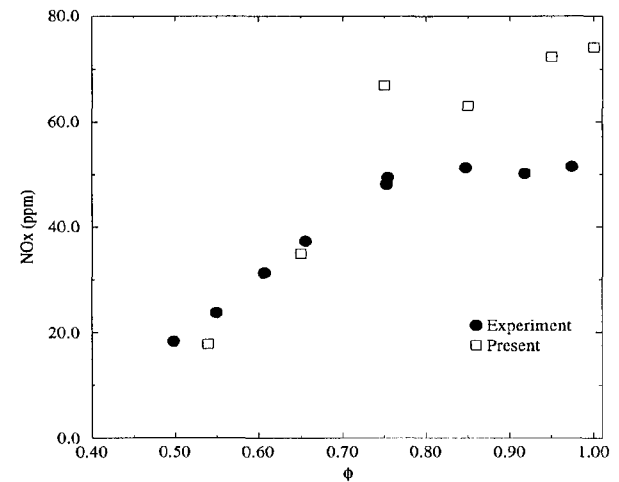


Fig. 12. NO mass fraction variation with ϕ . Measurements at X/D = 3.0 are shown.